

# Beneficial effects of retroreflective materials in urban canyons: results from seasonal monitoring campaign

**F Rossi, E Morini, B Castellani<sup>1</sup>, A Nicolini, E Bonamente, E Anderini, F Cotana**  
University of Perugia, Department of Engineering, CIRIAF, Via G. Duranti 67, Perugia,  
Italy, IT

E-mail: [beatrice.castellani@unipg.it](mailto:beatrice.castellani@unipg.it)

**Abstract.** Urban Heat Island (UHI) is a phenomenon that happens in urban areas consisting in higher temperatures than those in the surrounding rural areas. Cool materials and urban forestry have been identified as the mean countermeasures to this phenomenon. The specific research target was to investigate the benefit that can be obtained by the application of new retro-reflective (RR) cool materials on building envelopes in urban canyons. An ideal RR is a high reflective material that reflect incident radiation backward to the same direction of incidence. The test facility is made of two twin arrays resembling urban canyons with different aspect ratios. On the East array a cool, white, diffusive material is applied. On the West array a cool, white Retro-Reflective (RR) material is applied. The result of a seasonal (summer) monitoring campaign is discussed, with a particular focus on the temperature trends inside canyons with the same geometry but different envelope materials. While temperatures measured by the vertical sensors reveal a higher surface temperature of the RR, air temperatures and pavements' superficial temperatures are lower when RR are applied. These results suggest that RR materials have a cooling potential as coatings in urban canyons, and can thus improve urban climate conditions during summer.

## 1. Introduction

Urban Heat Island phenomenon (UHI) is related to higher temperatures in urban areas with respect to the suburban ones [1]. UHI is mainly given by urban facilities and human activities which contribute to urban temperature increase: buildings absorb daytime heat and release it at night-time; air conditioning, vehicles and industry release thermal heat; buildings decrease air flow; the lack of green spaces and the city pavements also increase absorption and storage of solar radiation [2]. UHI intensity depends on: geography, topography, climate, morphological and geometrical properties, materials, land-use and land-cover configuration, emission profiles and energy use [3]. Urban warming has negative effects on environmental and social aspects and affects the energy balance of the cities [4]. The main consequences are a significant increase of the peak and total electricity demand for cooling [5], a greater energy consumptions of several urban facilities as outdoor lighting [6] the worsening in thermal comfort in outdoor spaces and air quality conditions [7-10] and human health risks and increase of mortality [11]. Several researches also showed that the use of appropriate materials on the building envelope can have positive effects on the phenomenon mitigation and on the improvement of outdoor air quality and comfort conditions [12-14]. These materials are called "cool": cool roofs [15], cool pavements [16] and other innovative solutions including phase change materials [17] and thermochromic materials [18] are object of research. They are typically characterized by high solar reflectance (albedo) and high infrared emittance. Many studies show the positive effects of this relatively simple and cost-effective technique on urban heat island. It is well known and documented that a large scale change of albedo has a serious impact on the local peak ambient temperature [19]. It has been

<sup>1</sup> To whom any correspondence should be addressed.



demonstrated that increasing the albedo by 0.15 can reduce peak summertime temperatures by up to 1.5 °C in urban areas like Los Angeles [20]. In [21] through MM5 climate model two modified albedo scenarios have been compared to assess the effect of cool materials on the reduction of UHI in Athens: results show that temperature decreases up to 2.2 K. With a global climate model [22] it has been assessed the effects of albedo control on urban areas. The annual mean heat island decreased by 33%, the daily maximum and minimum urban temperature decreased respectively of 0.6° C and 0.3°C. Numerous studies also focused on the reduction of building energy consumption due to cool materials use [23-26]. During the DESIREX Campaign 2008 [27], it was stated that a higher albedo leads to about 5% reduction in energy consumption for air conditioning during summertime periods for the area of Madrid.

It has also been estimated that an increase of urban albedo (roofs and pavements) by 0.1 give a negative radiative forcing equivalent to offsetting 44Gt of CO<sub>2</sub> emission globally [28]. In [29,30] it has been demonstrated that 10 m<sup>2</sup> of high albedo surface can compensate 1 tCO<sub>2eq</sub> at Mediterranean latitudes.

Retro-Reflective (RR) materials are here proposed as new cool materials for UHI mitigation. RR is a high reflective material that reflects mostly the incident radiation in the same direction of the incoming radiation. RR materials have been recently proposed as cool materials [31]. The purpose of this paper is to investigate the benefits that can be obtained by the application of RR materials on building envelopes in urban canyons. The test facility, located at the University of Perugia (Italy) is made of two twin arrays resembling urban canyons with different aspect ratios [32]. On the east array a white diffusive material was applied while on the west array a white RR material is applied. The monitored temperatures in a cloudless, sunny summer day are discussed. The objective of the monitoring campaign is to compare the effect of two different types of cool materials, diffusive and RR, simultaneously during the same environmental conditions (solar irradiation, wind). Such analysis is based on the temperatures that are measured by the sensors of the facility and has a purely comparative significance. The improvement of cooling potential of retroreflective materials with respect to the white diffusive envelope is assessed.

## 2. The test field

The facility is composed of two twin arrays (West field and East field), each one representing two sets of canyons (Canyon 1, Canyon 2 and Canyon 3). Canyon 1, 2 and 3 are characterized by a H/D ratio of 1, 0.5 and 2 respectively. The facility, shown in Figure 1, is located on a roof enclosed by a 1-meter high stone parapet.



**Figure 1.** Experimental facility located at the University of Perugia.

In both the fields a bituminous membrane stands for a typical asphalt road on the horizontal surface. On the vertical surfaces of the canyons a white diffusive membrane (East field) and a RR membrane (West field) are installed. Optical characteristics of the investigated materials were assessed by spectrophotometric analysis. They are shown in Figure 2. Diffusive and RR materials basically differ from each other for their optical properties, in particular for the angular distribution of the reflected incident rays. An ideal diffusive surface is defined as a surface that reflects incident light in a hemisphere (a half disk in 2D). In this case thus energy is reflected by the surfaces towards all the directions, with an isotropic trend. An ideal RR surface, instead, is defined as a surface that reflects all the radiation toward the direction of incidence. The light is thus reflected in an ellipse whose major axis is in the direction of the incident radiation and its length depends on a  $\cos^n$

mathematical relation [33]. In light of this, the materials that were applied on the vertical surfaces of the facility have different behaviours and influences on the nearby surfaces.

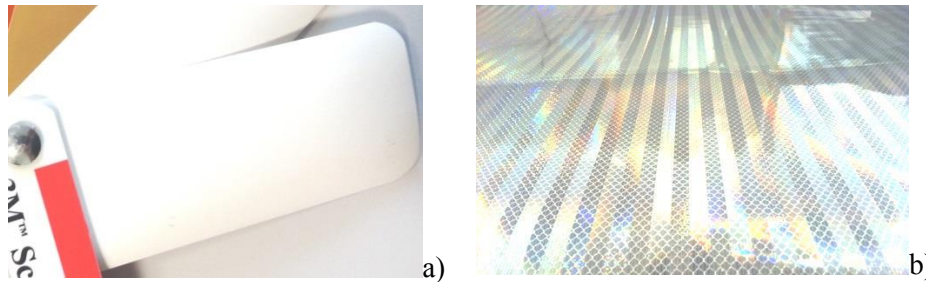


**Figure 2.** Investigated materials: a) white diffusive sample, b) retro reflective sample.

Temperature sensors are represented in Figure 3. “P” sensors measure the surface temperature of the pavement, “A” sensors measure the temperature of the air and  $V_S$  and  $V_N$  sensors measure the surface temperature of the vertical walls exposed to South and to North respectively. The same scheme is adopted for Canyons 1, 2, and 3 for both the West and East field. Temperature sensors are constituted by K-type thermocouples. The test field is also equipped with a meteorological station and an upward-facing pyranometer. The facility is not thought for dynamic similarity studies since fluid dynamic phenomena that take place inside the canyon are not under control. Therefore, results from the experimental investigation are just comparative but not scalable.

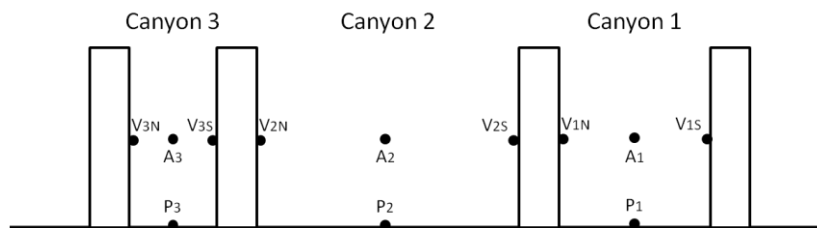


**Figure 3.** Scheme of the sensors inside the canyons. The same scheme is adopted for the East (white) and West (RR) field.

### 2.1. Spectrophotometric analysis of materials

Global reflected radiation profiles of RR and diffusive samples over the wavelength are reported in Figure 4.

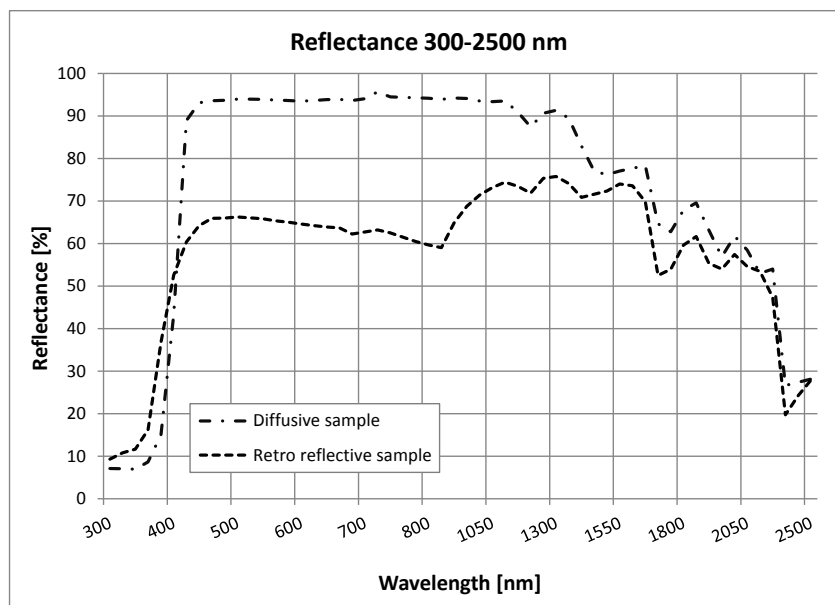


**Figure 4.** Reflectance spectrum of the samples.

Reflectance of the investigated materials in the solar spectrum is measured by Shimadzu SolidSpec 3700 spectrophotometer equipped with 60 mm integrating sphere. The spectrophotometer measurement range is 280–2500 nm, which includes the 99% of the solar energy. The value of solar reflectance is calculated as described in ASTM Standard G 173 [34,35]. The purpose of these measurements is the evaluation of the global hemispherical solar reflectance even in terms of spectral distribution. Solar reflectance measurements by the spectrophotometer show that the RR material has an overall reflectance equal to 62.8%, lower than that of the diffusive sample, equal to 86.5%. RR global reflectance in the range from 300 to 400 nm is higher than that of the diffusive film. In the infra red range RR global reflectance is much lower than that of diffusive material as well as in the visible spectrum.

### 3. Discussion of results

#### 3.1. Data analysis

A three-month monitoring campaign during summer 2014 was carried out in the test facility, located in Perugia. July 20<sup>th</sup> was chosen as reference hot sunny day to evaluate the effect of the RR material on the energy balance in the canyons. The maximum, minimum and average measured temperatures are about 34° C, 26° C, and 18° C respectively and levels of irradiation measured by the pyranometer are higher than 0.8 kW/m<sup>2</sup> for many consecutive hours throughout the day. Wind velocity measurements were lower than 2 km/h during the entire reference day. Wind intensity has surely an influence on temperature trends, also because fluid dynamic phenomena that take place inside the canyon are not under control. Optical properties of the investigated materials are not affected by outdoor conditions. In addition, both RR and diffusive materials are studied simultaneously and under the same climatic conditions, therefore the related temperature profiles are influenced to the same extent. This does not invalidate the experimental campaign characterized by a comparative approach. Temperature difference  $\Delta T$  was calculated as the difference between temperatures recorded by sensors in the East field and the West field respectively in each "n" position ( $\Delta T_n$ ). Since in the East field the vertical surfaces are white and in the West field the vertical surfaces are RR, a value of  $\Delta T > 0$  reveals that RR allow to reduce the energy absorbed, trapped and circulating in the canyons. The trend of  $\Delta T$  has been graphed for the n measurement points and the subtended areas have been calculated ( $A_{\Delta T, n}$ ). Since data are collected every 10 minutes, temperatures between two consecutive records were linearly interpolated.  $A_{\Delta T, n}$  was thus calculated as the sum of trapezoids, whose parallel sides are represented by the recorded temperatures. As for the  $\Delta T_n$  itself, a positive value of the subtended area means that energy in that point of the RR canyon is less than energy in the corresponding point of the white canyon.  $A_{\Delta T, n}$  values have been then compared with the areas subtended by the curves that represent the temperatures at the respective n position in the East field ( $A_{E, n}$ ). The percentage of energy trapped within the canyons saved by the RR material is thus showed in comparison with the energy trapped within the white canyons during six hours, to distinguish the daytime and the night-time savings. To consider the effect of the energy trapped during July 20<sup>th</sup> on night-time temperatures, the evaluations are carried out from July 20th at 00:00 to July 21st at 06:00. These evaluations have been treated separately for each measurement point in the canyons (pavement, air, vertical points) and finally a combined evaluation of the points belonging to the same canyon is presented. The results are shown below.

#### 3.2. Air temperature

Air temperature profiles inside canyons are shown in Figure 5. The represented profiles show very low differences between RR and diffusive material in all the three canyons. To better comment such results, temperature differences  $\Delta T_{A1}$ ,  $\Delta T_{A2}$ , and  $\Delta T_{A3}$ , related to Canyon 1, Canyon 2 and Canyon 3 respectively were calculated according to procedure in Paragraph 3.1. Profiles are shown in Figure 6.

As can be seen from the graphs, the maximum value of  $\Delta T$  occurs during the central part of the day, from 11:00 to 15:00, when solar irradiation is higher. Nevertheless, temperature differences oscillate rapidly from positive to negative values. Data are therefore organized and analysed on a 6-hourly basis and subtended areas are calculated. For the 6-hourly trends, Table 1 shows increases or reductions of trapped energy calculated as ratios between subtended areas of  $\Delta T$  profiles and subtended areas of diffusive materials' temperature profiles ( $A_{\Delta T, A}/A_{E, A}$ ). Negative values of  $\Delta T$  occur during night (from 00:00 to 05:50) in Canyon 1 and Canyon 3, both characterized by an higher H/D ratio than Canyon 2. This means that RR materials tend to increase nocturnal air temperatures in narrow canyons if compared to diffusive cool materials.

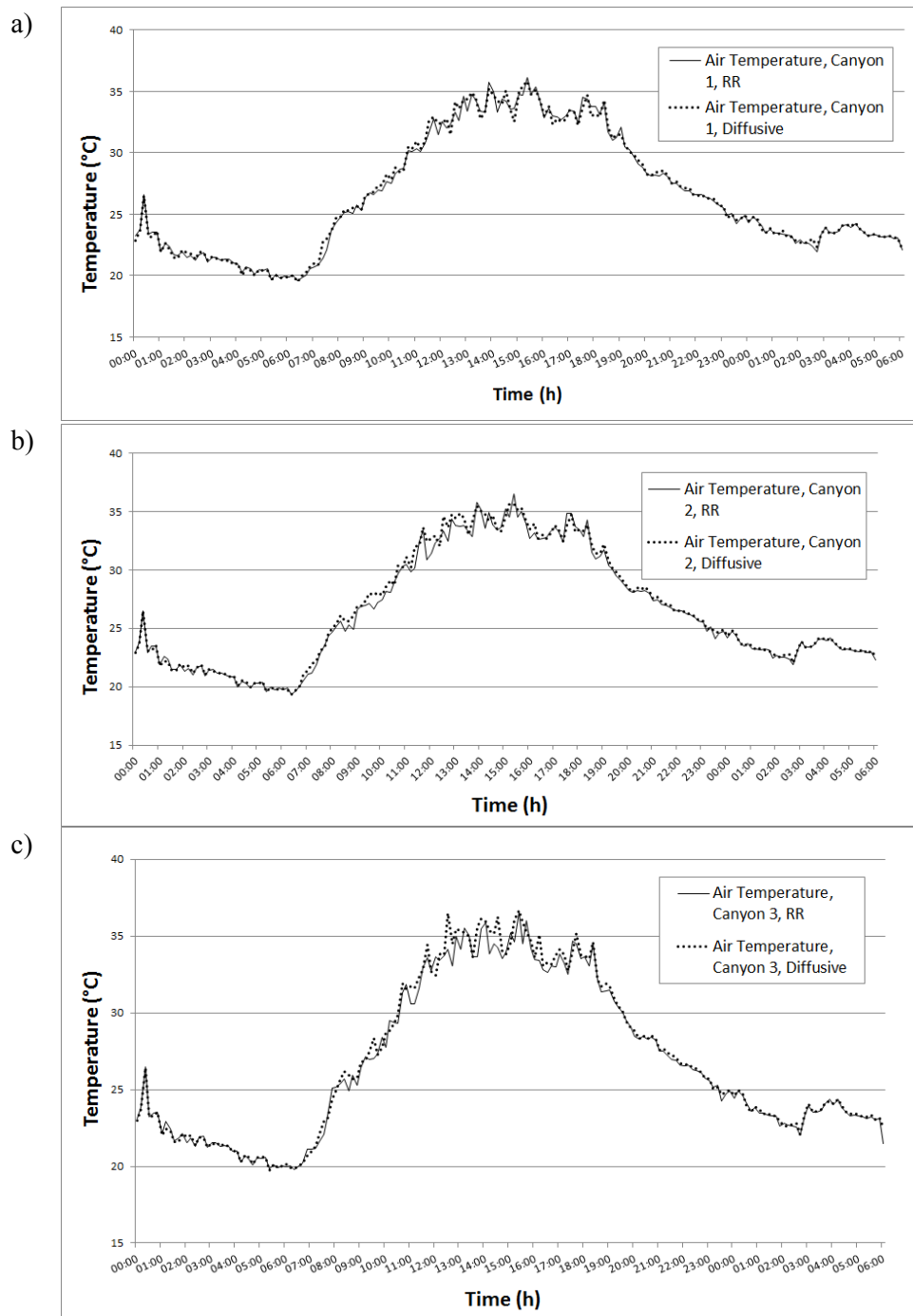


Figure 5. Air temperature profiles (A1, A2, A3): a) Canyon 1, b) Canyon 2, c) Canyon 3.

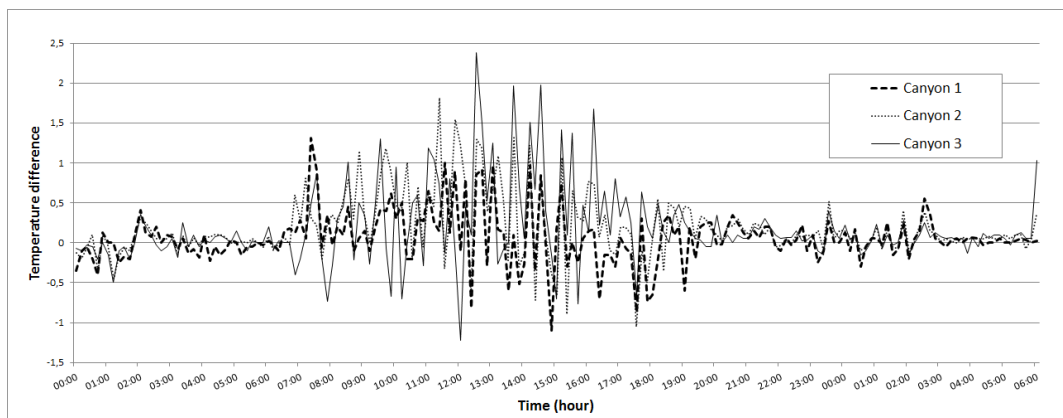


Figure 6. Differences of air temperature between RR and diffusive materials for the three canyons.

It is important to underline however that this negative effect is practically negligible since the increase of trapped energy is lower than 0.2%.

A cooling effect of RR materials can be observed during the central part of the day in all the three canyons with a reduction of energy trapped in the canyon equal to 1-2%.

**Table 1.** 6-Hourly trend of  $A_{AT,A}/A_{E,A}$  (%)

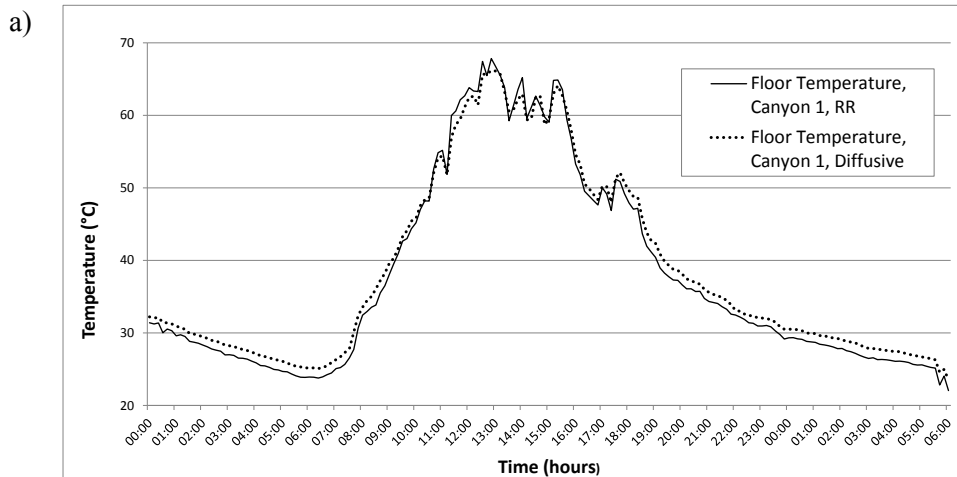
hours	$A_{AT,A1}/A_{E,A1}$ (%)	$A_{AT,A2}/A_{E,A2}$ (%)	$A_{AT,A3}/A_{E,A3}$ (%)
from 00:00 to 05:50	-0.179	0.024	-0.048
from 06:00 to 11:50	1.013	1.751	0.177
from 12:00 to 17:50	-0.0501	0.721	1.535
from 18:00 to 23:50	0.002	0.606	0.436
from 24:00 to 06:00	0.162	0.305	0.329

The global effect of RR materials during the entire reference day (24 hours) is quantified equal to 0.23% (for  $A_1$ ), 0.71% (for  $A_2$ ) and 0.68% (for  $A_3$ ) avoided energy. This reveals a lower energy trapped in the RR canyons at temperature air level, with respect to energy trapped in the white diffusive canyons.

### 3.3. Pavement temperature

Pavement superficial temperature profiles are shown in Figure 7. Temperature differences on pavements are more marked, especially for Canyon 2 and Canyon 3 in the central part of day, showing a pronounced cooling effect of RR materials. In the same period, RR and diffusive materials in Canyon 1 show the same effect on temperatures. During night time, temperatures of diffusive pavements are slightly higher than those of RR pavements. Differences of pavement superficial temperature between RR and diffusive materials measured at P1, P2 and P3 points are shown in Figure 8. It can be noticed that temperatures of RR pavements are always lower than temperatures of diffusive pavements during the entire reference day. The maximum difference in the range of [3-7] °C occurs during the hottest hours of the day. Temperatures of the pavements, lower in the RR Canyons can be explained recalling what have been stated before about the optical properties of the vertical surfaces. The RR material reflects backward to the incidence direction the most of the incoming radiation and just a little radiation towards the other directions. The diffusive one, instead, diffuses the reflected radiation on its typical hemisphere and in an isotropic way. This justifies the higher temperatures of the pavements in the diffusive Canyons, that are struck by the direct radiation and also by reflected waves.

Data are then analyzed in accordance with procedure in Paragraph 3.1 on 6-hourly basis and shown in Table 2. The hourly comparison reveals savings up to 6.77%, 7.57% and 6.74% in  $P_1$  and  $P_2$  from 06:00 to 11:50 am, and in  $P_3$  from 12:00 to 17:50 pm respectively. As shown in Figure 7, two negative percentages are found in  $P_2$  from 00:00 to 05:50 am and from 18:00 to 23:50 pm. The daily comparison reveals savings of 5.15%, 2.41% and 5.27%, showing an RR global cooling effect on canyon's pavements.



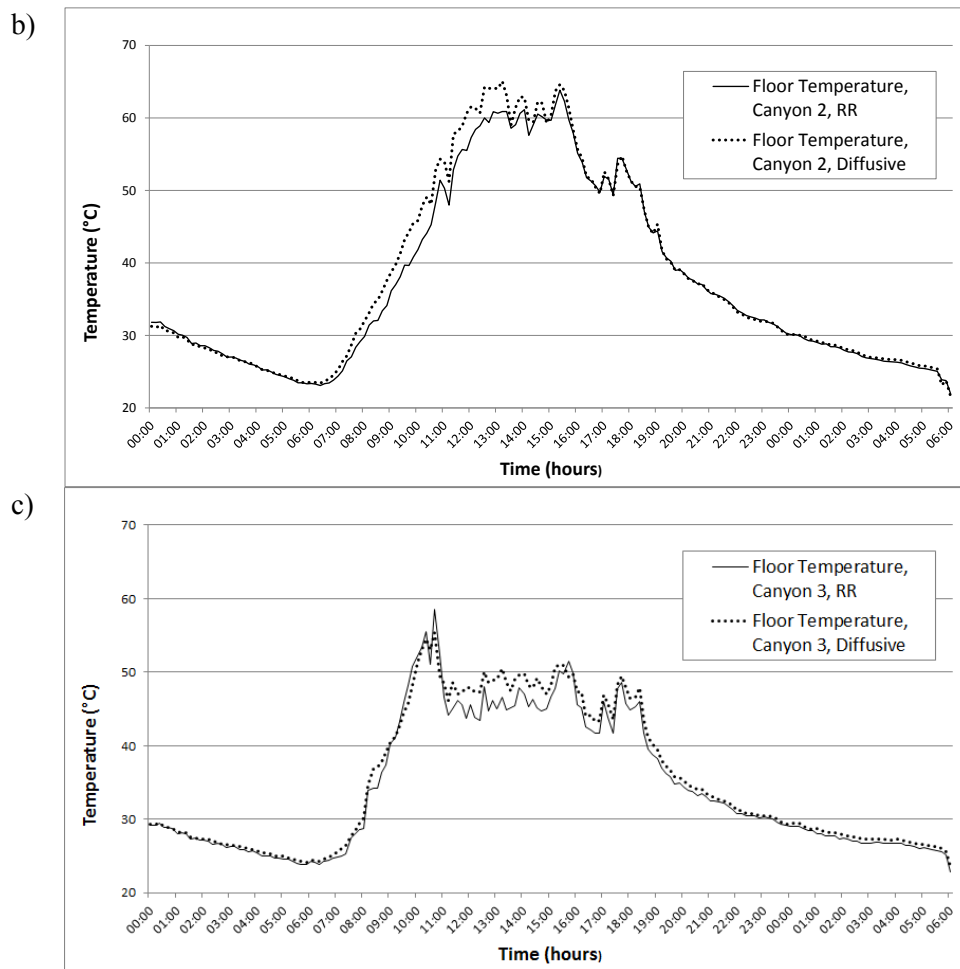


Figure 7. Pavement superficial temperature profiles: a) Canyon 1, b) Canyon 2, c) Canyon 3.

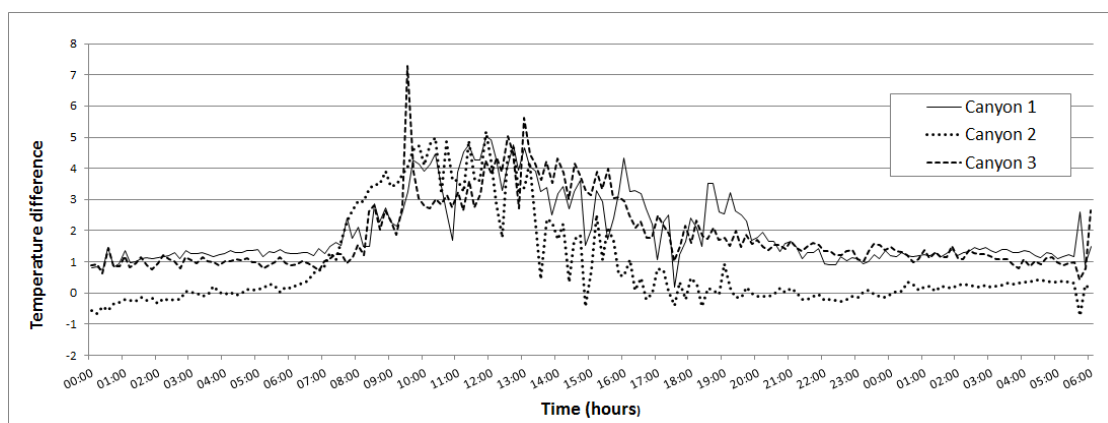


Figure 8. Differences of pavement superficial temperature between RR and diffusive materials for the three canyons.

Table 2. 6-Hourly trend of  $A_{AT,P}/A_{E,P}$  (%)

hours	$A_{AT,P1}/A_{E,P1}$ (%)	$A_{AT,P2}/A_{E,P2}$ (%)	$A_{AT,P3}/A_{E,P3}$ (%)
from 00:00 to 05:50	4.205	-0.369	3.733
from 06:00 to 11:50	6.771	7.572	1.638
from 12:00 to 17:50	5.103	2.530	6.739
from 18:00 to 23:50	0.045	-0.065	4.444
from 24:00 to 6:00	4.635	0.825	4.163

### 3.4. Façades temperatures

Façades have been treated separately, according to their exposition.

#### 3.4.1. South-oriented façades

Superficial temperature profiles on south-oriented façades are shown in Figure 9. For all the three canyons, temperatures during the central part of the day are higher in case of RR materials. During night time, results of comparison are not uniform: in Canyon 1 temperature trends overlap, in Canyon 2 RR materials show higher temperatures while in Canyon 3 they have lower temperatures.

Differences of south-oriented façades temperature between RR and diffusive materials measured at  $V_{1s}$ ,  $V_{2s}$  and  $V_{3s}$  points are shown in Figure 10. Profiles reveal many positive values for  $\Delta T$  but also many large negative values, with peak negative values at 10:50 ( $\Delta T = -5.82$  °C), 12:20 ( $\Delta T = -7.68$  °C), and 12:20 ( $\Delta T = -5.66$  °C) for  $V_{1s}$ ,  $V_{2s}$ , and  $V_{3s}$  respectively.

According to this trend, the percentage of energy reveals that up to a 3.8% extra of energy is absorbed by the vertical surfaces exposed towards South in the RR canyon than in the white one.

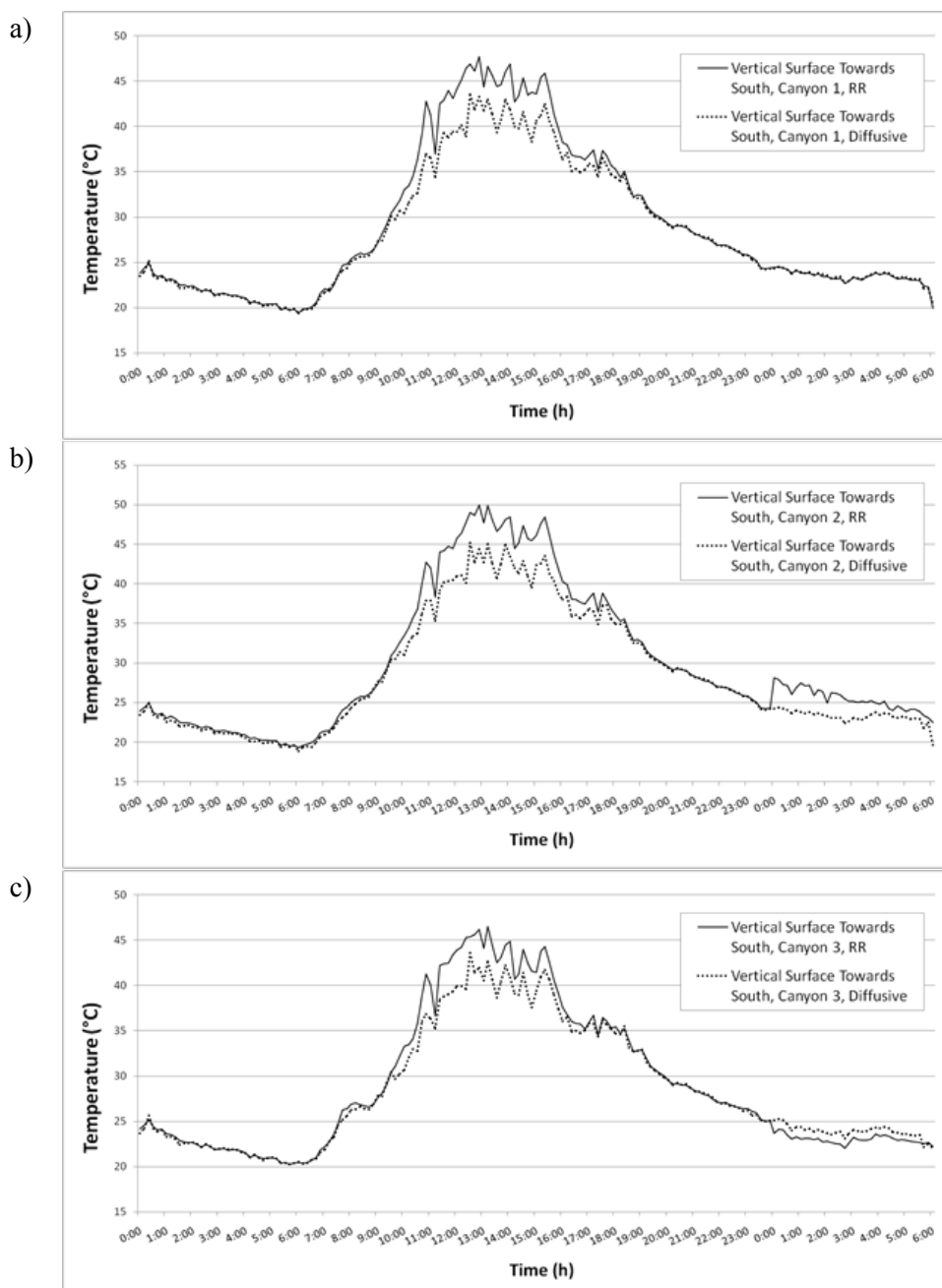
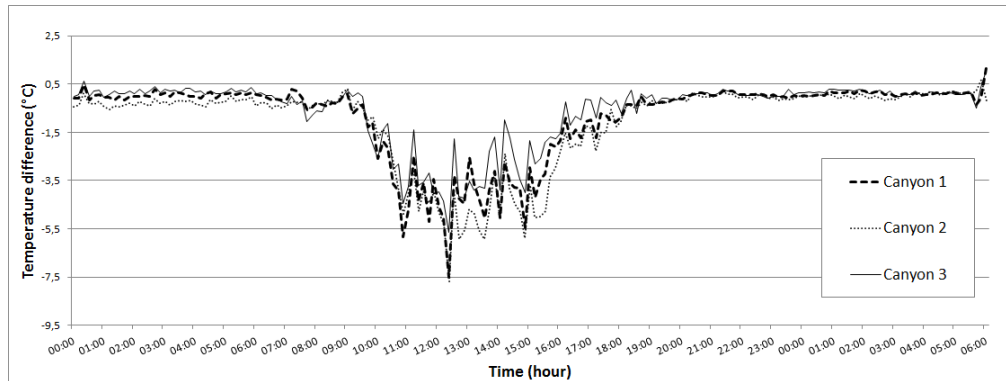


Figure 9. South-oriented façades' temperature profiles: a) Canyon 1, b) Canyon 2, c) Canyon 3.

Values of  $A_{\Delta T,VS}/A_{E,VS}$  are -3.070 for V1s, -3.794 for V2s and -2.130 for V3s. On 6-hourly basis, the percentage of extra energy kept into the canyon is up to about 7%, 9% and 6% in the middle hours of the day (Table 3). Data show a negative effect of RR materials on energy absorbed by south-oriented façades. The worst behaviour is observed in Canyon 2, the flattest one.



**Figure 10.** Differences of south-oriented façade superficial temperature between RR and diffusive materials for the three canyons.

**Table 3.** 6-Hourly trend of  $A_{\Delta T,VS}/A_{E,VS}$  (%)

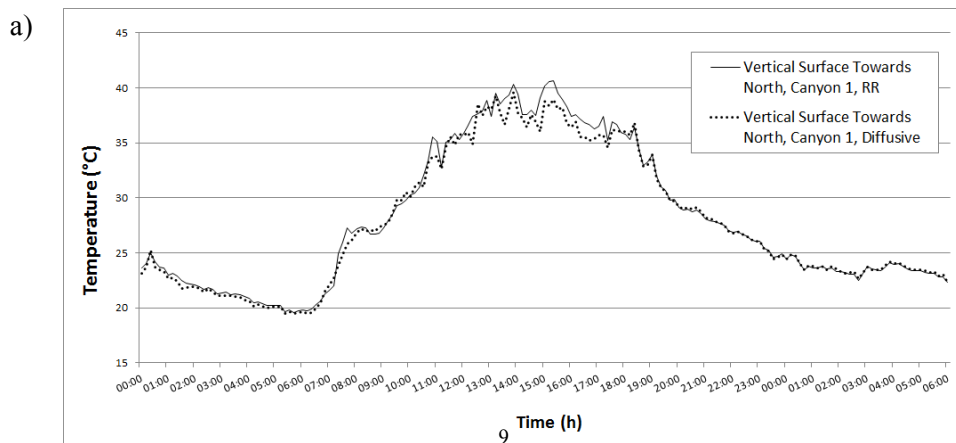
hours	$A_{\Delta T,VS1}/A_{E,VS1}$	$A_{\Delta T,VS2}/A_{E,VS2}$	$A_{\Delta T,VS3}/A_{E,VS3}$
from 00:00 to 05:50	0.190	-1.262	0.863
from 06:00 to 11:50	-5.149	-4.966	-1.082
from 12:00 to 17:50	-7.653	-9.042	-5.587
from 18:00 to 23:50	-0.002	-0.437	0.027
from 24:00 to 6:00	0.526	0.214	0.682

#### 3.4.2. North-oriented façades

Superficial temperature profiles on north-oriented façades are shown in Figure 11. Differences between RR and diffusive materials are not as sharp as in the south-oriented vertical surfaces analysed before.

Temperature differences between RR and diffusive materials measured at  $V_{1N}$ ,  $V_{2N}$  and  $V_{3N}$  points are shown in Figure 12. Profiles reveal many positive values for  $\Delta T$  and many large negative values. The peak positive values are 1°C, 0.5°C and 1.8°C in canyon 1, canyon 2 and canyon 3 respectively. The peak negative values are -3.9°C, -2.9°C, -2.4°C in canyon 1, canyon 2 and canyon 3 respectively. The overall daily effect of RR is an increase, although minor (up to 1%), of the energy that is held in the canyon. Values of  $A_{\Delta T,VN}/A_{E,VN}$  are -0.594 for  $V_{1N}$ , -1.093 for  $V_{2N}$  and -0.045 for  $V_{3N}$ .

On 6-hourly basis, this increase is up to 2%, 2.7% and 0.7% in canyon 1, 2, and 3 respectively from 12:00 to 17:50 (Table 4). The increase of superficial temperature is due to an overall lower level of reflectance of RR materials with respect to a white diffusive material.



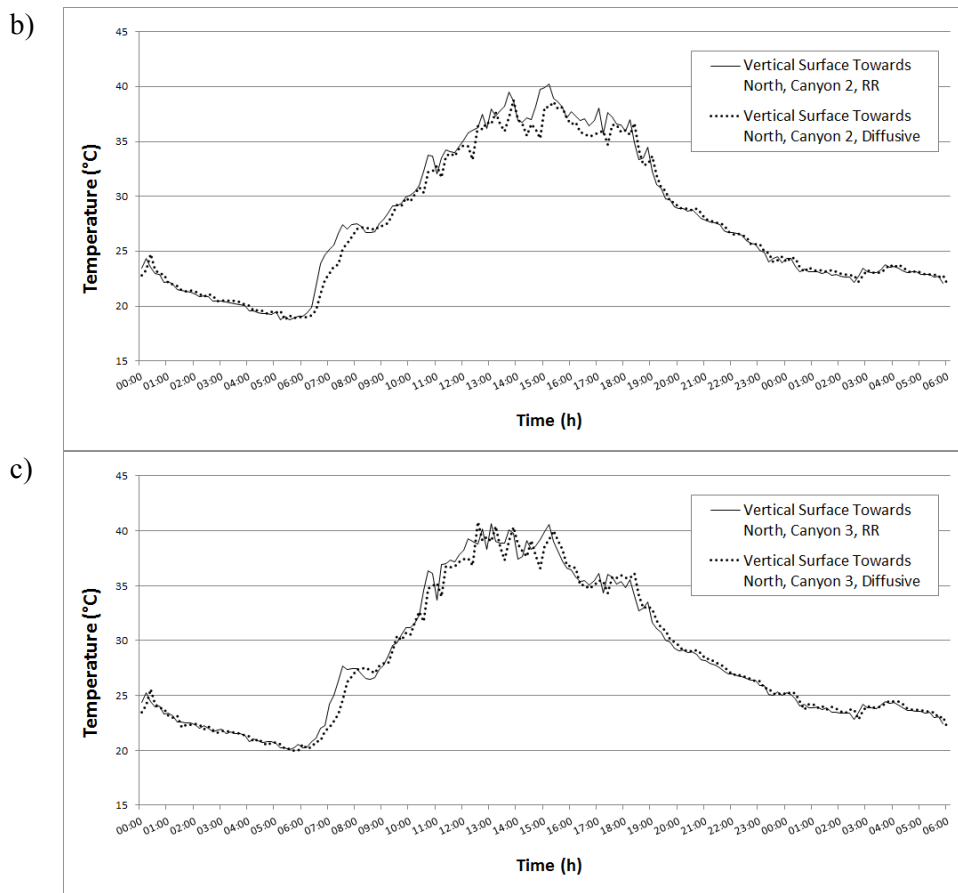


Figure 11. North-oriented façades' temperature profiles: a) Canyon 1, b) Canyon 2, c) Canyon 3.

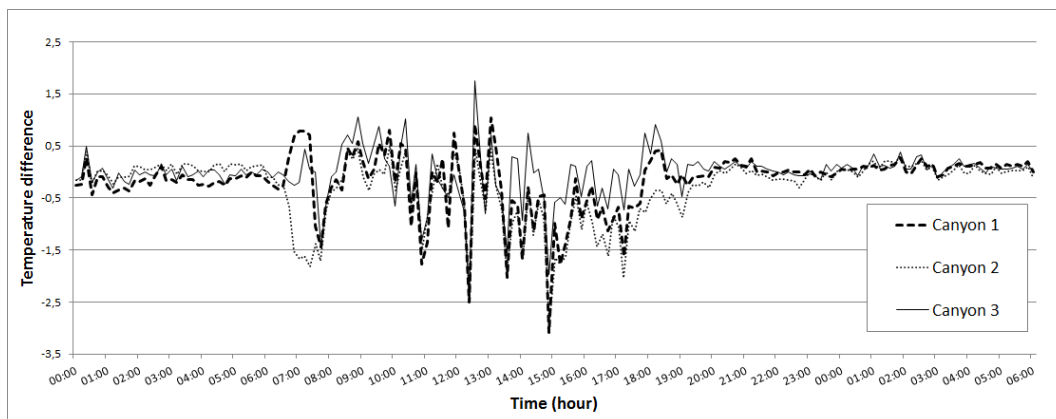


Figure 12. Differences of north-oriented façade superficial temperature between RR and diffusive materials for the three canyons.

Table 4. 6-Hourly trend of  $A_{AT,VN}/A_{E,VN}$  (%)

hours	$A_{AT,VN1}/A_{E,VN1}$	$A_{AT,VN2}/A_{E,VN2}$	$A_{AT,VN3}/A_{E,VN3}$
from 00:00 to 05:50	-0.787	0.207	-0.168
from 06:00 to 11:50	-0.216	-1.515	0.005
from 12:00 to 17:50	-1.984	-2.764	-0.686
from 18:00 to 23:50	0.001	-0.623	0.315
from 24:00 to 6:00	0.468	0.270	0.551

The main disadvantage of RR materials is related to the temperatures measured by the vertical sensors, that reveal a higher surface temperature of the RR on the façades. On the other hand, the decrease of the air and ground temperature reveal its UHI mitigation potential. In addition, the effect of RR materials on energy trapped in the canyon depends strictly on the geometry of the canyon itself. In particular the cooling potential of the investigated RR coating on air temperature is evident in Canyon 2, that is the flattest one. A lower air temperature is associated to higher façades' superficial temperatures as shown in Table 4.

#### 4. Conclusions

The trend of temperatures in three urban canyons on a scale test facility with H/D ratio equal to 1, 0.5 and 2 has been analyzed. A comparative analysis about the influence of a retro-reflective (RR) material with respect to a white diffusive cool material applied on vertical surfaces of urban canyons has been treated. The comparative analysis is based on temperatures' trend: a positive  $\Delta T$  and a positive area subtended by  $\Delta T$  reveals a benefit from the RR compared to the white material. An individual evaluation for air, vertical surfaces and horizontal surfaces reveal benefits and disadvantages from RR materials. The main disadvantage is related to the temperatures measured by the vertical sensors, that reveal a higher surface temperature of the RR. Solar reflectance measurements by the spectrophotometer show indeed that the RR material has an overall reflectance equal to 62.8%, lower than that of the diffusive sample, equal to 86.5%. The temperature measured by air temperature sensors and the temperature measured by pavement sensors, and thus the urban heat island effect, decreased in the RR canyons. As for the air temperature a decrease up to 1% is measured. As for the pavement temperature a much higher reduction of temperature is registered: the reduction is between 5% and 22% in canyon 1, between 1% and 2% in canyon 2, and between 5% and 10% in canyon 3 at night-time (from 00:00 to 06:00). These results suggest that RR materials have a cooling potential with respect to traditional white diffusive coatings in urban canyons, and can thus improve urban climate conditions during summer. The evaluations provided in this paper are based on a comparative analysis between the performance of an RR material and a white diffusive material. The validation for real scale application will be object of the next steps of the research. The extension of the present evaluations to real scale is foreseen. With this purpose, a dimensional analysis and similitude will be elaborated to correlate the above experimental results to real scale applications.

#### 5. References

- [1] Santamouris M 2001 James and James Science Publishers
- [2] Oke TR, Johnson DG, Steyn DG, Watson ID 1991 *Boundary-Lay Meteorol* **56** 339
- [3] Mihalakakou G, Flocas HA, Santamouris M, Helmis CG 2002 *J. Appl. Meteorol.* **41** 519
- [4] Santamouris M 2014 On the energy impact of urban heat island and global warming on buildings *Energy and Buildings* **82** 100
- [5] Asimakopoulos DA, Santamouris M, Farrou I, Laskari M, Saliari M, Zanis G, Giannakidis G, Tigas K, Kapsomenakis J, Douvis C, Zerefos SC, Antonakaki T, Giannakopoulos C 2012 *Energy Build.* **49**
- [6] Rossi F, Bonamente E, Nicolini A, Anderini E, Cotana F 2015 *Energy and Buildings* In press doi:10.1016/j.enbuild.2015.04.054
- [7] Pantavou K, Theoharatos G, Mavrakis A, Santamouris M 2011 *Building and Environment* **2** 339
- [8] Pantavou K, Theoharatos G, Santamouris M, Asimakopoulos 2013 *Building and Environment* **66** 82
- [9] Sarrat C, Lemonsu A, Masson V, Guedalia D *Atmos. Environ.* **40** 1743
- [10] Stathopoulou E, Mihalakakou G, Santamouris M, Bagiorgas HS 2008 *J. of Earth Syst. Scie.* **117** 227
- [11] Santamouris M, Kolokotsa D *Energy and Buildings* **98** 125
- [12] Akbari H, Matthews HD *Energy and Buildings* **55** 2
- [13] Santamouris M, Synnefa A, Karlessi T 2011 *Solar Energy* **85** 3085
- [14] Pisello AL, Rossi F, Cotana F 2014 *Energies* **7** 2343
- [15] Joudi A, Svedung H, Bales C, Rönnelid M 2011 *Appl Energy* **88** 4655
- [16] Levinson R, Pan H, Ban-Weiss G, Rosado P, Paolini R, Akbari H *Appl Energy* **88** 4343
- [17] Castellani B, Morini E, Filippini M, Nicolini A, Palombo M, Cotana F, Rossi F *Sustainability* **6** 6815
- [18] Doulos L, Santamouris M, Livada I 2004 *Solar Energy* **77** 231
- [19] Synnefa A, Santamouris M, Livada I 2006 *Solar Energy* **80** 968
- [20] Oleson KW, Bonan GB, Feddema J 2010 *Geophysical Research Letters* **L 37** 03701
- [21] Kolokotroni M, Ren X, Davies M, Mavrogianni A 2012 *Energy and Buildings* **47** 302
- [22] Kolokotsa D, Diakaki C, Papantoniou S, Vliissidis A *Energy Build* **55** 85
- [23] Santamouris M *Solar Energy* **103** 682

- [24] Zinzi M, Carnielo E, Agnoli S 2012 *Energy Build* **50** 111
- [25] Salamanca F, Martilli A, Yague C 2008 *International Journal of Climatology* **32** 2372
- [26] Campra P, Garcia M, Canton Y, Palacios-Orueta A 2008 *J.of Geophysical Research* **D113** 18109
- [27] Taha H 1997 *Energy and Buildings* **25** 99
- [28] Akbari H, Menon S, Rosenfeld A 2009 *Climatic Change* **95** 3
- [29] Rossi F, Cotana F, Filipponi M, Nicolini A, Menon S, Rosenfeld A 2013 *Adv. Build. En.Res.* **7** 254
- [30] Cotana F, Rossi F, Filipponi M, Coccia V, Pisello AL, Bonamente E, Petrozzi A, Cavalaglio G 2014 *Applied Energy* **130** 641
- [31] Rossi F, Castellani B, Presciutti A, Morini E, Filipponi M, Nicolini A, Santamouris M 2015 *Applied Energy* **145** 8
- [32] Bonamente E, Rossi F, Coccia V, Pisello AL, Nicolini A, Castellani B, Cotana F, Filipponi M, Morini E, Santamouris M 2013 *Advances in building Energy Research* **7** 222
- [33] ASTM E903-12. Standard test method for solar absorptance, reflectance, and transmittance of materials using integrating spheres.
- [34] ASTM G 173-03. Standard tables for reference solar spectral irradiances: direct normal and hemispherical on 37° tilted surface; 2012.
- [35] Rossi F, Pisello AL, Nicolini A, Filipponi M, Palombo M 2014 *Applied Energy* **114** 621